Estimation of Pre-Post Surgical Changes in the fMRI Visual Field Map

Raymond G. Hoffmann[1], Thomas J. Hoffmann[2], Edgar A. Deyoe[3], Daniel B. Rowe[4]
[1]Biostatistics, Medical College of Wisconsin, Milwaukee, WI, 53226
[2]Biostatistics, Harvard University,
[3]Radiology Research, Medical College of Wisconsin
[4]Biophysics, Medical College of Wisconsin

Abstract

The visual field map is produced by activating the visual cortex in the brain with a dynamic visual target presented to the subject.s right eye. The activated regions are then mapped to a circular region corresponding to the points of the circular target. It is a dynamic option to the Humphries map that ophthalmologists use to evaluate visual acuity.

SA 1: To detect whether there has been a change in the Visual Field map due to a surgery or disease.

SA 2: To determine an estimated probability map of where the change has occurred

KEY WORDS: fMRI, spatial, point process

1. The Visual Field Map Generates a Point Process

The visual field diagram is formed by an inverse mapping of areas of the visual cortex to the retinotopic area stimulated by an array of visual targets.

A series of circular annulus (doughnuts with a hole), expanding out from the center of the target plus a series of pie-shaped wedges rotating around the circular target are used to map the location on the retina to the location in the visual cortex. As can be seen from the map of the visual cortex below, homogeneous regions of the cortex correspond to homogeneous portions of the retina – identified by the same color (red to yellow to green to blue corresponding to the inner part of the retina expanding to the outermost annulus of the retina).

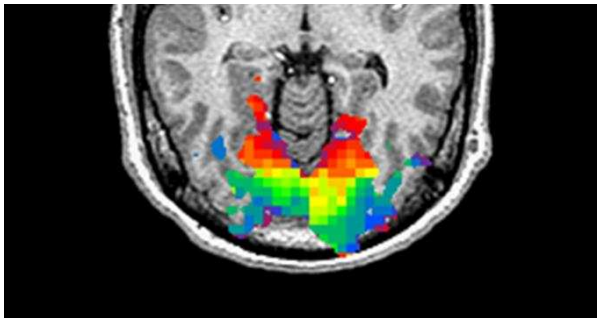

Figure 1.1. The Visual Cortex (Deyoe, 1996)

Figure 1 shows the functional activation of the cortex with the visual field eccentricity (the distance from center of gaze) represented by different colors calculated from the delay of the fMRI signal.

The FFmap, like the retina of the eye is spatially inhomogeneous. There are more receptors near the center of vision which allows more sensitivity.There are 450 to 650 points in a Visual Field

2. Simulated Effects of Surgery

The visual target that is used to obtain the FFmap is composed of two parts. The first is a semicircular (180 degree) checkerboard pattern that rotates around a 360 degree circle. In order to "simulate" the effect of surgery, a wedge was cut out of the semicircular pattern. The second part of the target was a set of annuli (rings around the center of the visual field) that went from the center out to the edge of the fisual field. Wedges were used to mask part of the visual field when the data was collected from a subject. The wedges were 0, 18, 27, 36, 45 and 90 degrees.

Noise in the signal may cause mapping to the wrong place. Moreover, a voxel is large enough so that it may actually span more the veins that correspond to one one sector. So even though it may correlate with more than one spot, only is one is designated as activated.

Because of the "**winner take all"** rule for assigning activation, when the voxel spans two different regions, the noise involved in a real fMRI signal results in a map that has random points in the area of the wedge.

The number of points designated as active, depends on the threshold of activation. Thus, the number of points in the area masked by the wedge may be "improved" by adjusting the threshold at which a point is declared active. However, this is not a useful procedure, because it requires knowing where the problem occurs before one looks for it.

Thus the method used to identify visual abnormalities will have to take into account that fMRI signals do not have an absolute reference.

3. Analytic Methods

3.1 A Critique of Methods for Assessing Changes in Spatial Patterns

There are several methods for identifying changes in spatial point patterns. Most of them rely on the assumption that the points come from a spatially homogeneous Poisson process. Some of the methods used are as follows:

- Using a spatial distance measure between (1) the point and the nearest neighbour for each point or (2) a random location and the nearest point has poor sensitivity. For example, using the c.d.f of the nearest neighbor distances, F(d) together with a Kolmologorov-Smirnov test of the differences between the distributions is Sensitive to thinning, but insensitive to sections cut out.
- Comparing an expected (pre-surgery) number of points in an area with an observed number of points (post-surgery) with a chi-square goodness of fit test has too many false positives because of the problem of adjusting for the potential change in threshold value between fMRI scans.
- Fitting a spatial point process model to the data will be explored in this paper.

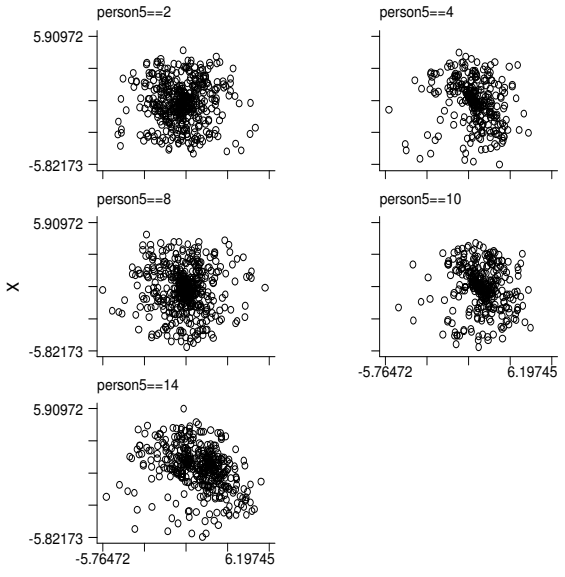

Figure 3.1
Repeated observations of the same subject at different sessions with no masking, but the same threshold. The maps have 479, 295, 588, 428 and 619 points, respectively.

3.2 Models for the Point Process

The usual model for a point process assumes an underlying density with constant intensity. Often this is modeled with a homogeneous Poisson process.

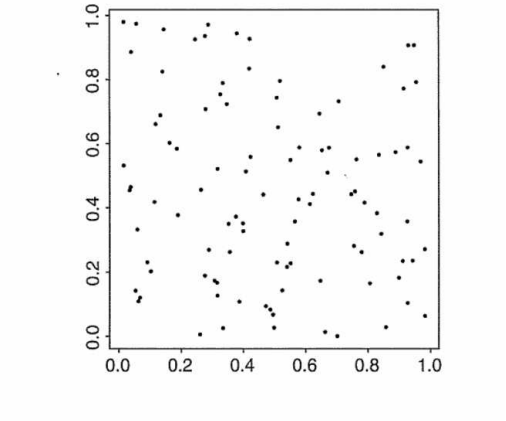

Figure 3.2
A homogeneous Poisson process with a constant intensity λ.

A homogeneous Poisson process will have a constant intensity λ. It will not have a uniformly spaced set of points; it will have a pattern that looks like figure 3.2. A uniformly spaced set of points must have a repulsion factor in the model to keep the points from getting too close.

3.3 The Poisson Spatial Point Process

The homogeneous Poisson process, $\lambda(s) = \lambda$, where s is any point in the visual field.

Given the total number of events N_k occurring within an area A, the N_k events represent an independent random sample of N locations, with the probability of sampling a particular point s_i proportional to λ

3.4 Modeling the First Order Intensity

$\lambda(s)$ is the first order or mean of the spatial process. A homogeneous Poisson Process has $\lambda(s) = \lambda$

Since the visual field is not uniform, the point process needs to be non-homogeneous. Choosing an underlying model for the intensity, $\lambda(s)$, is not easy. A particular problem is that the intensity is not monotone away from the center because of visual features like the blind spot (the optic nerve in the retina).

However, smoothing the pre-surgical observed data can give an empirical (person-specific) model to test against.

3.5 An Empirical Intensity Estimate

The intensity is not monotone away from the center because of visual features like the blind spot (the optic nerve in the retina). We can smooth the **empirical densities** of each of the visual field maps. An example of the smoothed empirical densities is shown in figure 3.5 for a 0 degree mask, a 45 degree mask and a 90 degree mask.

The effect of the masks can be seen both on the area that is masked out as well as the effect that it has on the central, most dense region. The central region is actually split up into two or more smoothed peaks by the mask. However, making a quantitative comparison of the empirical point process densities is difficult. Primarily this is because there are multiple smoothing and window parameters that must be chosen to obtain the empirical density. Trying to smooth the ratio of the two densities is equally demanding in terms of the number of parameters that must be specified.

The difficulty with smoothing is that there are many parameters to choose: Window size, kernel type, and grid on which the result is plotted and displayed

The results are VERY sensitive to bandwidth, Results are also moderately sensitive to alignment across sessions, but tend to overshoot near the center The kernel type is not very important We used the R library splancs for smoothing kernels and estimating ratios of smoothed kernels

3.6 Using the Full Scan to estimate the Predicted Point Density

An alternative solution to trying to compare empirical densities is to use a Poisson Process model for the Visual Field Map. The data forms a point process. A point appears if it is above a (correlation) threshold.

$$\{ Y(s_i): \ i = 1, \ldots N_k \}$$

where $Y(s_i) = 1$ and
s_i is the location of the point

A spatial point process model has an intensity function

$$\lambda(x) = \lim \left\{ \frac{E[N(dx)]}{|dx|} \right\} \text{ as } |dx| \to 0$$

Which will be constant for a homogeneous process

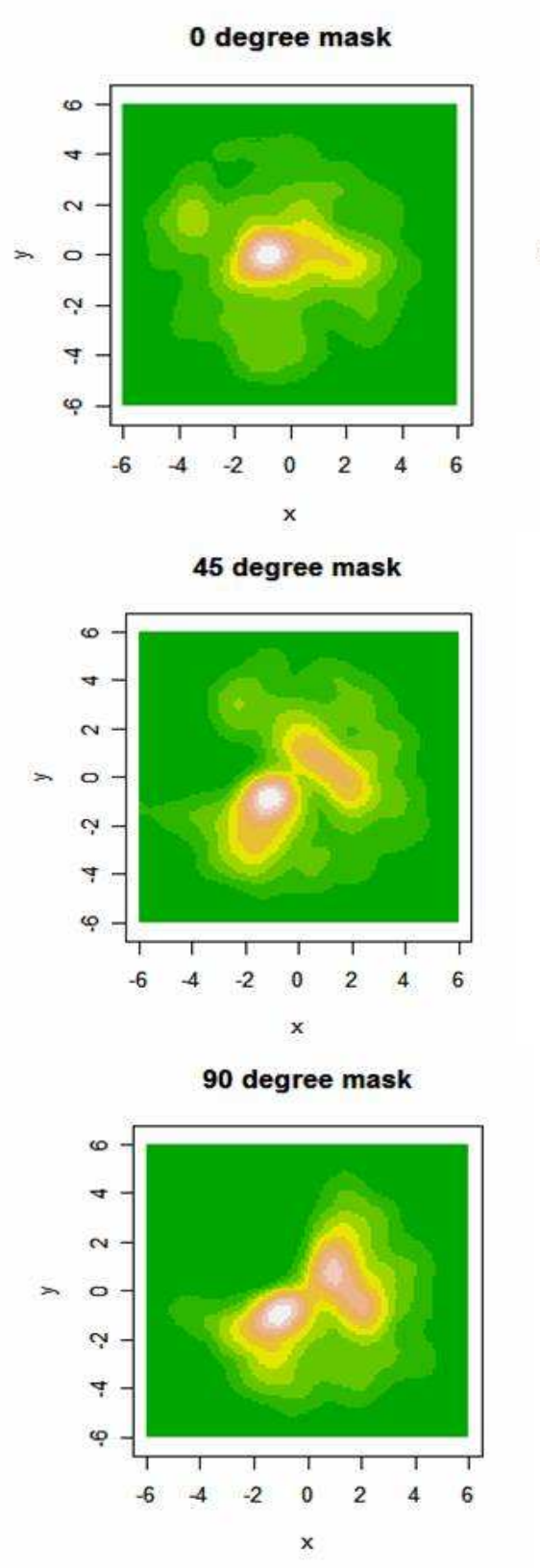

Figure 3.5
Emprically smoothed densities for different masks.

The number of the events occurring within a finite region A is a random process following a Poisson distribution with mean

$$\int_A \lambda(s)ds$$

Thus the process doesn't need to be homogeneous, but can actually be non-homogeneous.

Given the total number of events N_i occurring within an area A, the N events represent an independent random sample of N locations, with the probability of sampling a particular point s_i proportional to $\lambda(s)$

A non-homogeneous Poisson Process model for the Visual Field Map for s=(x,y)

$$\lambda(x,y) = \exp\{\mu + \alpha_1 x + \alpha_2 x^2 + \beta_1 y + \beta_2 y^2\}$$

to model the decrease in the intensity of the process moved away from the center (0,0) of the eye. The parameters α_2 and β_2 allow the process to be anisotropic**.**

3.7 Using a Parametric Model for the First Order Intensity

Comparing the densities with a non-homogeneous Poisson Process model for the Visual Field Map gives a model for the point s=(x,y). The simplest model will decrease smoothly as one moves away from the center of the visual field, the center (0,0) of the eye. The simplest model is

$$\lambda(x,y) = \exp\{\mu + \alpha_1 x + \alpha_2 x^2 + \beta_1 y + \beta_2 y^2\}$$

will model a smooth decrease in the intensity as the process moves away from (0,0). The parameters α_2 and β_2 allow the process to be anisotropic (directional), which is a natural characteristic of the visual field. However, the actual visual field is not that smooth.

In order to model the effect of the wedge changing the shape of the curve as well as allowing for innate asymmetry even without a wedge, we included additional terms:

$$\lambda(s) = \exp\{\mu + \alpha_1 x + \alpha_2 x^2 + \beta_1 y + \beta_2 y^2 + \beta_3 x^2 y^2 + \gamma_1 xy + \gamma_2 x^2 y + \gamma_3 xy^2\}$$

The interaction terms γ_1, γ_2 and γ_3 should be near zero for the 0 degree mask, but become more positive or negative in value when there is a region that is masked. In other words, we are modeling the effect of any defect in the visual field by an increase in the asymmetry terms of the model.

3.8 Bootstrap Estimate of the Variance of the γ's

The estimation of the coefficients is only useful if we also can estimate the variability of these coefficients. Then we will be able to test whether there has been a significant change in the point process as mirrored in the intensity:

$$\lambda(s) = \exp\{\mu + \alpha_1 x + \alpha_2 x^2 + \beta_1 y + \beta_2 y^2 + \beta_3 x^2 y^2 + \gamma_1 xy + \gamma_2 x^2 y + \gamma_3 xy^2\}$$

There at least two methods for performing the resampling to estimate the variance of γ's by using bootstrap resampling.

i) Resample N_k points from the N_k points in the data set

ii) Generate N_k points from the empirically smoothed estimate of density from N_0,

4. Computational Methods

To fit the intensity for the non-homogeneous Poisson process, we used R and the **spatstat** library for the spatial Poisson process.

The full mask was compared to a 90 degree mask and a 45 degree mask**.** The interaction was modeled with three terms:

- A linear interaction term
- A quadratic x trend and linear y
- A quadratic y trend and linear x

The intensity trend formula for the spatial Poisson process was

~ x + I(x^2) + y + I(y^2) + I(x^2*y^2)

+ I(x * y) + I(x^2 * y^2) + I(x * y^2)

250 naïve bootstrap replications were programmed in R to estimate the variance of each of the masks.

5. Results

A 3D projection of the fitted intensity to the visual field map with no mask is shown in figure 5.1.

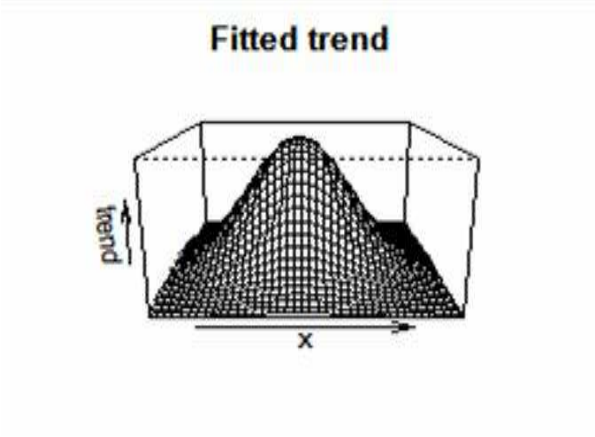

Figure 5.1

In order to see how the fitted curves correspond to the observed points a contour map of the fitted density is overlaid with the observed points. Figure 5.2 shows the results for the 0 degree and the 90 degree masks. Figure 5.3 shows the results for the 45 degree mask.

The tables show the comparison of the estimated coefficients for the 90 degree masked (Bnw90), the 45 degree masked (Bnw45) and the unmasked (Bnw00), and their bootstrap variances.

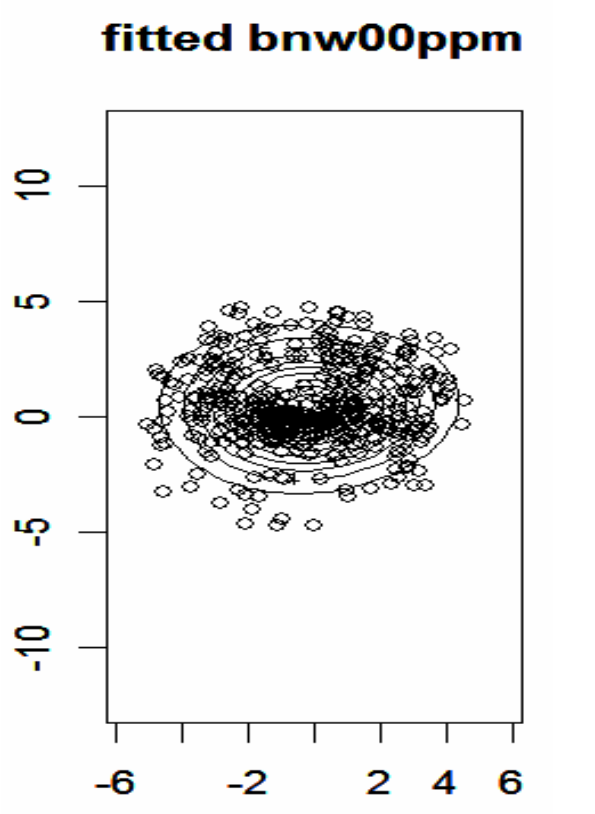

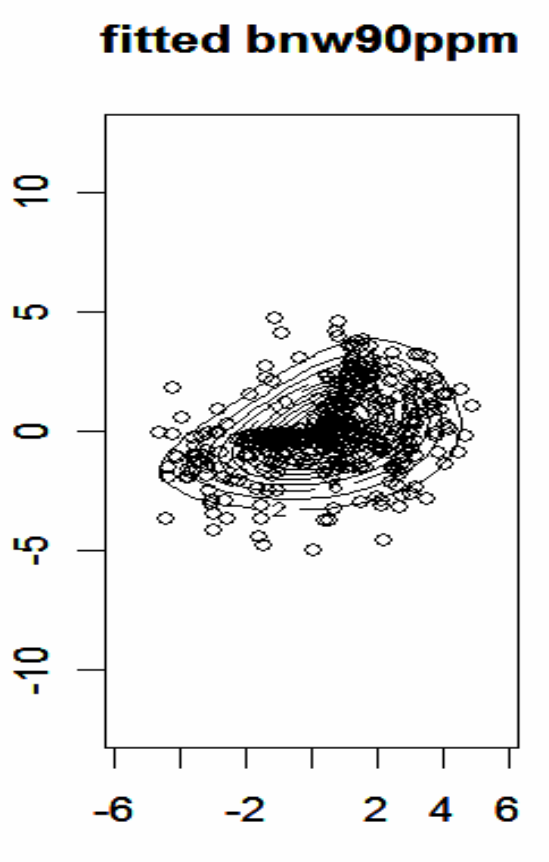

Figure 5.2
The 0 and 90 degree masks

We also tested a 45 degree wedge cutout. Which was quite a bit more difficult to detect.

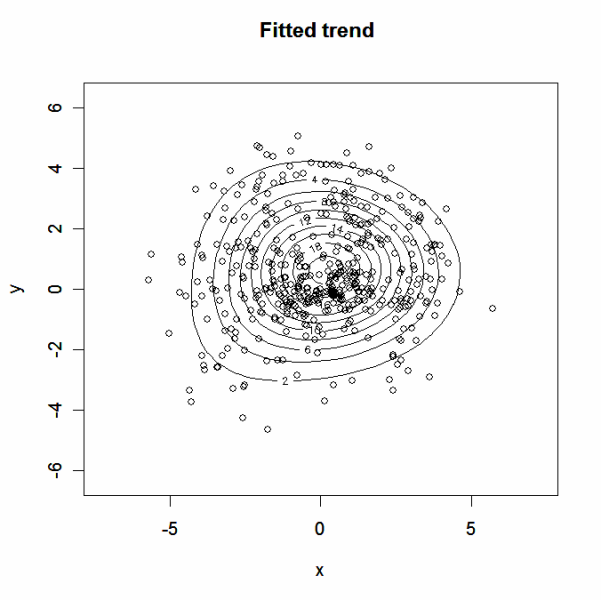

Figure 5.3
The 45 degree mask.

The Poisson process model was fit using the R spatstat library for the spatial Poisson process. 250 naïve bootstrap replications were programmed in R to estimate the variance.

Term	Bnw00	Bnw90
Intercept	3.0437 (.063)	3.1957 (.064)
X	-0.0416 (.0365)	0.1354 (.0365)
Y	0.1217 (.0343)	-0.0347 (.0393)
I(X^2)	-0.1173 (.0099)	-0.1522 (.0126)
I(Y^2)	-0.1809 (.0174)	-0.2454 (.0270)
I(X * Y)	**0.0126 (.0155)**	**0.1906 (.0331)**
I(X * Y^2)	**-0.0035 (.0061)**	**0.0339 (.0142)**
I(X^2 * Y)	**0.0046 (.0046)**	**-0.0355 (.0094)**
I(X^2 * Y^2)	0.0006 (.0020)	-0.0052 (.0036)

The tables show the comparison of the estimated coefficients for the 90 degree masked (Bnw90), the 45 degree masked (Bnw45) and the unmasked (Bnw00), and their bootstrap variances.

Term	Bnw00	Bnw45
Intercept	3.0437 (.063)	2.9654 (.060)
X	-0.0416 (.0365)	0.0304 (.0289)
Y	0.1217 (.0343)	0.2281 (.0301)
I(X^2)	-0.1173 (.0099)	-0.1162 (.0100)
I(Y^2)	-0.1809 (.0174)	-0.1823 (.0156)
I(X * Y)	**0.0126 (.0155)**	**0.0284 (.0155)**
I(X * Y^2)	**-0.0035 (.0061)**	**0.0137 (.0059)**
I(X^2 * Y)	**0.0046 (.0046)**	**-0.0069 (.0038)**
I(X^2 * Y^2)	0.0006 (.0020)	-0.0017 (.0019)

Using a parametric model for the intensity improves both the sensitivity and specificity of identifying a wedge shaped defect.

Open questions:

- How does it work with holes?
- How robust is it to model choice, e.g. cox process, etc.
- Using a bootstrap/model that includes the between scan sampling variability.

6. Future Directions

A Bayesian non-parametric model using a 2D Dirichelet prior may be the most adaptive to the individual subject, as well as answering the clinical question "The posterior probability that the difference observed at any location is due to surgery is"
The Empirically Smoothed figures suggest that another way to model the change in shape when a segment is removed from a VFD is to use a (Gaussian) mixture model that will have more than one peak (like a mountain range) as the size of the wedge increases.

Acknowledgements

National Center for Research Resources (NCRR) grant RR00058General Clinical Research Center. We thank Mary Jo Maciejewski for the sample data that we used to illustrate the use of the model.

References

Brefczynski J, DeYoe EA. "A physiological correlate of the 'spotlight' of visual attention" Nature Neuroscience 4: 370ff. , 1999

DeYoe, E. A., G. Carman, et al. (1996). "Mapping striate and extrastriate visual areas in human cerebral cortex." Proceedings of the National Academy of Sciences - USA 93(6): 2382-2386.

DeYoe, E. A., K. Williams, et al. (1997). "FMRI-based "functional field maps" of brain-related vision defects." Society for Neuroscience Abstracts 23: 1403.

Diggle P. Statistical Analysis of Spatial Point Patterns. 2nd ed. Oxford. U. Press. 2001.

Hoffmann RG, Macjewski MJ, Savarapian P, DeYoe EA, Rowe DB. " Methods for Assessing Changes in the Visual Field Map after Surgery", Statistical Computing Section, American Statistical Association, 2006.

Rowe DB. Hoffmann RG. Multivariate statistical analysis in fMRI. *IEEE Engineering in Medicine & Biology Magazine*. 25(2):60-4, 2006.

Schabenberger O and Gotway CA. Statistical methods for Spatial Analysis. 2004. CRC Press.